Inherited Carboniferous to Permian zircons constrain the continuity of the Gondwanan continental arc beneath the central Chilean Andes (32-34° S)

*Katja Deckart[1], Abigail Jackson-Gain[1], Kei Sato[2], Luisa Pinto L.[1], Mauricio Calderón[3]

[1]*Departamento de Geología, FCFM, Universidad de Chile. Plaza Ercilla 803, Santiago, Chile.* kdeckart@cec.uchile.cl, abbyjackson.gain@gmail.com, lpinto@uchile.cl

[2]*Instituto de Geociências, CEP 05508-080 Universidade de São Paulo, Brazil.* *keisato@uspr.br*

[3]*Facultad de Ingeniería, Universidad del Desarrollo. Av. Plaza 680, Las Condes, Santiago, Chile.* mccaldera@gmail.com

*Corresponding author:

ABSTRACT

This study investigates the crustal architecture and tectonomagmatic evolution of the central Chilean Andes (32-34° S) through new U-Pb zircon geochronology. Results from the western border of the Principal Cordillera (32-33° S) reveal a dominant late Carboniferous to early Permian inherited signature, accounting for 60-62% of zircon populations in Late Cretaceous and Miocene units. The high frequency of these Paleozoic ages confirms an unexposed crustal basement, while their incorporation into younger magmas is attributed to the Pocuro Fault system, interpreted as the northern extension of the deep-seated West Andean Thrust (WAT), acting as a conduit for crustal material at least for the Miocene intrusive rocks. Notably, the near-total absence of Mesoproterozoic (Grenvillian) inheritance in these samples suggests that the Cuyania and Chilenia blocks (Grenvillian basement) do not constitute the immediate basement at these latitudes. In the Coastal Cordillera (34° S), the Pailimo Unit yielded a primary magmatic age of 299.2±1.6 Ma without older inherited components, aligning with the entire magmatic belt of south-central Chile (33-40° S). Collectively, these data indicate that the Gondwanan magmatic arc forms a laterally contiguous lithospheric framework extending from the Coastal to the Frontal Cordilleras. This research highlights a major geodynamic transition from a Paleozoic subduction-accretion system toward a mature Andean-type margin. The results underscore the necessity for further integrated studies along the western Gondwana margin.

Keywords: Western Gondwana margin, Carboniferous-Permian magmatism, U-Pb geochronology, Coastal Batholith, Central Depression-Principal Cordillera section.

RESUMEN

Este estudio investiga la arquitectura cortical y la evolución tectonomagmática de los Andes chilenos centrales (32-34° S) mediante nuevos datos geocronológicos U-Pb en circón. Los resultados de la zona de transición morfoestructural (32-33° S) revelan una firma heredada dominante del Carbonífero tardío al Pérmico temprano, que representa entre el 60% y el 62% de las poblaciones de circones en unidades del Cretácico Tardío y Mioceno. La alta frecuencia de estas edades paleozoicas confirma la presencia de un basamento cortical inferior, mientras que su incorporación en magmas más jóvenes se atribuye al sistema de Fallas Pocuro, interpretado como la extensión septentrional de la falla profunda *West Andean Thrust* (WAT), actuando como un conducto para material cortical, al menos durante el Mioceno. En estas muestras destaca la ausencia casi total de herencia mesoproterozoica (tipo Grenvilliano), lo que sugiere que los bloques de Cuyania y Chilenia (basamento Grenviliano) no constituyen el basamento inmediato en estas latitudes. En la Cordillera de la Costa (34° S), la Unidad Pailimo arrojó una edad magmática primaria de 299.2±1.6 Ma sin componentes heredados más antiguos, lo cual se alinea con el cinturón magmático más amplio del centro-sur de Chile (33-40° S). En conjunto, estos datos indican que el arco magmático de Gondwana constituye un marco litosférico lateralmente contiguo que se extiende desde la Cordillera de la Costa hasta la Cordillera Frontal. Esta investigación destaca una transición geodinámica mayor desde un sistema de subducción-acreción paleozoico hacia un margen maduro de tipo andino. Los resultados subrayan la necesidad de realizar más estudios integrados a lo largo del margen occidental de Gondwana.

Palabras clave: Margen occidental de Gondwana, Magmatismo Carbonífero-Pérmico, Geocronología U-Pb, Batolito costero, Depresión Central-Cordillera Principal.

1. Introduction

The southwestern Gondwana margin during the Gondwanan orogeny (Carboniferous-early Permian) is relevant for the understanding of how extensive and simultaneously diverse a convergent margin can be. Carboniferous-early Permian intrusive rocks can be found throughout the Pacific margin of Chile (e.g., Hervé et al., 1988, 2014; Maksaev et al., 2014; del Rey et al., 2016; Creixell et al., 2021, 2025) and Argentina (Moreno et al., 2020; Dahlquist et al., 2021; Rocher et al., 2024; Santos da Cruz et al., 2024), notably 21-40° S (Fig. 1). In Chile, manifestations of subduction-related late Carboniferous igneous and metamorphic rocks are seen at 21° S and 32° S at the limit between the Coastal Cordillera and the Principal Cordillera (e.g., Ramos and Folguera, 2009; Álvarez et al., 2011; Maksaev et al., 2014), as well as farther south between 33° S and 38° S within the Coastal Cordillera (e.g., Willner et al., 2005; Deckart et al., 2014; Jorquera et al., 2023). In addition, eastward magmatic migration is recorded near 40° S along the western margin of the Principal Cordillera, extending into the Liquiñe-Ofqui Structural System (Deckart et al., 2014). In Argentina, at around 41-42° S, the Plutonic Guillelmo-Serrucho Complex and the El Platero Tonalite (Pankhurst et al., 2006; Rossel et al., 2024) have also been attributed to this same subduction-related Gondwanan event. Yet farther south, Devonian to early Carboniferous igneous rocks crop out in northern Patagonia, related to earlier tectonic scenarios (e.g., Pankhurst et al., 2003; de la Cruz and Suarez, 2006; Hervé et al., 2016; Rapela et al., 2021; Marcos et al., 2023; Rossel et al., 2024; Renda et al., 2025), and in southern

Patagonia, Tierra del Fuego (Mella and Quiroz, 2023). The southernmost connection with the herewith studied areas remains unresolved.

A remarkable amount of tectonic, geochemical, and geochronological information for these rocks is available for different spatial sections of the Gondwana margin (e.g., Parada et al., 1990; Ramos and Folguera, 2009; Deckart et al., 2014; Hervé et al., 2014; Hyppolito et al., 2014; Maksaev et al., 2014; Heredia et al., 2018; del Rey et al., 2019; Creixell et al., 2025), but until now, no Carboniferous-early Permian rocks have been recorded at latitudes 32-33° S at the western border of the Principal Cordillera.

The primary objective of this study is to evaluate the magmatic continuity between late Carboniferous-early Permian calc-alkaline and peraluminous plutonism (21-32° S) and the contemporaneous metaluminous Coastal Cordillera Batholith (33-40° S). To support the temporal and spatial persistence of this magmatic system along the western margin of Gondwana, we present three new U-Pb zircon datasets. One is a concordia age of a biotite-hornblende diorite from the Coastal Cordillera Batholith (34°17' S). As for the other two, one comes from a granodioritic intrusive body and the other from a crystalline tuff, collected along the western border of the Principal Cordillera (between 32°29′ S and 32°42′ S), and characterized using relative-age probability analyses of inherited zircon populations. The latter two samples belong to the Pocuro Fault system, a long-lived tectonic boundary between the Principal and Coastal Cordilleras (e.g., Rivano et al., 1993; Estay et al., 2023; Charrier et al., 2024). These age data provide new insights into the role of this fault system in the inheritance and transport of Paleozoic crustal material within the modern tectonic framework (Figs. 1-3).

2. Contextual frame

2.1. Geodynamic context

Rodinia was a Proterozoic supercontinent composed of several major continental blocks, which fragmented at the end of the Mesoproterozoic (Weil et al., 1998; Cawood, 2005). The subsequent tectonic evolution of the proto-Andean margin has been interpreted in different ways. In the classical model, the breakup of Rodinia led to the formation of a single continental block referred to as Chi-Cu by Heredia et al. (2016), which later evolved into the individual tectonic blocks of Cuyania and Chilenia of mainly Mesoproterozoic (Grenvillian) age (Ramos, 1988), initially separated by the Chanic Ocean during the early Cambrian (Davis et al., 2000). Their accretion to the western margin of Gondwana occurred in two principal stages: first, the collision of Cuyania during the Famatinian orogeny (Early Ordovician–Silurian) (Ramos, 1988; Pankhurst et al., 1988; Pankhurst and Rapela, 1998; Vaughan and Pankhurst, 2008), followed by the collision of Chilenia during the Chanic orogeny (Middle Devonian-early Carboniferous), which resulted in the closure of the Chanic Ocean and the development of the Cuyania-Chilenia suture (Davis et al., 2000; Heredia et al., 2017).

An alternative interpretation proposed by Rapela et al. (2016) redefined this tectonic framework by questioning the existence of Chilenia as a distinct crustal block. Instead, the basement of the Western Sierras Pampeanas is interpreted as part of the MARA block, a predominantly Paleoproterozoic continental domain that underwent extensive tectonothermal reworking during the Grenvillian orogeny. In this framework, the widespread Mesoproterozoic-Grenvillian ages and isotopic signatures traditionally used to support the presence of a Chilenian or Grenvillian crustal component are interpreted primarily as evidence for the reworking of older continental crust, rather than for the existence of a separate Grenvillian terrane. Importantly, the distinctive detrital-zircon age distributions identified in the Western and Eastern Sierras Pampeanas demonstrate that zircon populations can serve as fingerprints of contrasting crustal domains, even where their basement is poorly exposed. Accordingly, the occurrence of Grenvillian-age signatures along the proto-Andean margin has been interpreted as evidence for a significant contribution from Mesoproterozoic-reworked continental crust to the basement of the western Gondwana margin. However, whether such a Grenvillian-influenced basement constituted the principal crustal component beneath the Central Andes at 32-33° S remains an open question.

Today, these Grenvillian-bearing basement rocks are exposed between ~27° S and ~38° S within the Frontal Cordillera of Argentina and Chile and in the Western Sierras Pampeanas, including the Sierra de Maz (e.g., Ramos, 1988, 2009, 2010; Chernicoff and Zappettini, 2004; Rapela et al., 2010; Varela et al., 2011). They comprise mainly mafic to ultramafic lithologies with a strong Laurentian-Grenvillian affinity and crystallization ages of ca. 1200-1030 Ma (Rapela et al., 2010; Varela et al., 2011). Whether interpreted as the basement of the Cuyania-Chilenia blocks or as part of the MARA block, these rocks represent the inherited continental crust upon which subsequent Andean tectonomagmatic evolution developed.

Following the final amalgamation of the western continental basement to the western Gondwana margin, subduction along the proto-Pacific margin commenced at about 320 Ma (late Carboniferous) or even slightly before (ca. 340-335 Ma, early Carboniferous) as suggested by Willner et al. (2005), Hyppolito et al. (2014), Creixell et al. (2021), and Dahlquist et al. (2025). This timing is consistent with the development of a Carboniferous arc domain in Argentina between 28° S and 30° S, encompassing the present-day Western Sierras Pampeanas and Frontal Cordillera, where arc-related magmatic rocks yield ages between 357±2 and 322±5 Ma (Dahlquist et al., 2021). These ages provide independent evidence for the onset of proto-Pacific arc magmatism during the early Carboniferous. The initiation of subduction marked the onset of the principal Gondwanan orogenic cycle (late Carboniferous-early Permian; Cawood, 2005; Cawood and Buchan, 2007), which was accompanied by widespread intrusive magmatism along the proto-Andean margin between 21° S and 40° S. This Carboniferous-early Permian magmatic system provides the regional tectonic framework for the present study (Fig. 1).

2.2. Geological context

The two samples, LP04 and CA06, collected slightly north of 33° S, are respectively situated within a geological framework dominated by stratified Cretaceous volcano-sedimentary successions (Cerro Morado, Las Chilcas, and Lo Valle formations), exposed predominantly in the Eastern Coastal Cordillera, and stratified Cenozoic volcano-sedimentary successions (Abanico and Farellones formations) that characterize the Principal Cordillera (Fig. 2; Jackson-Gain, 2023). These two morphostructural domains are separated by the ~N-S trending Pocuro Fault system (Fig. 2), a major structural boundary marking the western edge of the Andean orogen. To the south, this megastructure continues as the West Andean Thrust (WAT), a west-vergent structural system of reverse faults, inverted normal faults, and folds (e.g., Armijo et al., 2010; Ammirati et al., 2022), possibly active since at least the Eocene when de Abanico Basin started its development (Charrier et al. 2024). Sample LP04 is a crystalline tuff collected from the Upper Cretaceous Lo Valle Formation at Resguardo de Los Patos, adjacent to the Pocuro Fault system. Sample CA06 is a granodioritic intrusive rock from the Miocene Campos de Ahumada intrusion, emplaced within the Pocuro Fault system, where it intrudes the lower part of the Las Chilcas Formation (Fig. 2).

South of 33° S, the geological framework of the Coastal Cordillera Batholith, including the area surrounding sample N2204 (Figs. 1 and 3), is characterized by a Paleozoic metamorphic basement that has been interpreted as a late Paleozoic accretionary prism and paired metamorphic belt (Willner et al., 2005, 2008; Hervé et al., 2013). This basement is intruded by the Carboniferous-Permian plutonic complexes investigated in this study, as well as by younger Mesozoic plutonic bodies associated with the proto-Andean magmatic arc (Sernageomin, 2003). This crystalline foundation is unconformably overlain by Cenozoic marine sedimentary sequences. The structural architecture is characterized by ~NW-SE striking faults, which controlled the spatial distribution of some local hydrothermal activity and the configuration of the modern drainage system (Sernageomin, 2003).

3. Petrography

Three samples were analyzed: a crystalline tuff (LP04), a granodiorite (CA06), both collected along the present-day boundary between the Coastal and Principal cordilleras defined by the Pocuro Fault system (Fig. 2) (Rivano et al., 1993, 1996; Estay et al., 2023), and a biotite-hornblende diorite (N2204) from the Coastal Cordillera Batholith.

Sample LP04 (32°29’11” S, 70°36’38” W; Fig. 2) was collected at Resguardo de Los Patos, approximately 38 km north of Los Andes, on the western side of the Pocuro Fault system. Stratigraphically, it belongs to the Upper Cretaceous Lo Valle Formation (Thomas, 1958). The rock is a crystalline tuff with a pyroclastic texture with 50% lithic or crystalline fragments. Primary minerals are plagioclase (15%), K-feldspar (20%), quartz (5%), and opaque minerals (10%). The matrix is composed mainly of quartz and plagioclase, with varying proportions. The feldspars display an imbricated arrangement, indicating directional flow during deposition. The sample is generally characterized by significant chlorite and some epidote alterations principally affecting the feldspar group.

Sample CA06 (32°42’49” S, 70°32’59” W; Fig. 2) was collected from the Campos de Ahumada area, approximately 19 km north-northeast of Los Andes. It is a medium-grained granodiorite with a phaneritic texture, composed mainly of quartz (70%), biotite (5%), K-feldspar (15%), plagioclase (7%), and opaque minerals (3%).

Chlorite alteration is affecting the feldspar group and biotite, suggesting post-crystallization hydrothermal processes and meteorization effects.

Sample N2204 (34°17’13” S, 71°47’07” W; Fig. 3) is a biotite-hornblende diorite from the northern segment of the Coastal Cordillera, about 25 km northeast of Pichilemu. It corresponds to the Pailimo Intrusive unit, recognized as part of the Carboniferous-Permian Intrusive Complex, which comprises diorites, granites, granodiorites, and tonalites (Gana et al. 1996; Hervé et al., 2007). Sample N2204 is holocrystalline with phaneritic texture. Primary mineralogy is plagioclase, biotite, hornblende, quartz, K-feldspar, and some visible accessory zircon. Secondary minerals are calcite, epidote, and chlorite, primarily altering hornblende. Intracrystalline deformation is observed in quartz, evidenced by undulatory extinction, while biotite displays kink bands with a preferential orientation. A weak foliation mainly affects hornblende and biotite crystals.

4. Analytical methodology

4.1. Sample preparation

Mineral separation was carried out at the JV Circones y Minerales SpA facilities in Santiago using standard procedures, including crushing of about 2 kg of rock sample, followed by gravity gold panning, heavy liquids, and magnetic separation. Zircon crystals selected for geochronological analysis were handpicked under binocular microscopes. These crystals were then sent to two laboratories for U-Pb dating: the LA-ICP-MS Geochronology Laboratory at MQ GeoAnalytical, Department of Earth and Environmental Sciences, Macquarie University, Sydney, Australia (GEMOC) (samples LP04 and CA06), and the SHRIMP U-Pb Geochronology Laboratory at the Institute of Geosciences, University of São Paulo, Brazil (IGc-USP) (sample N2204). Age interpretation was used after Cohen et al. (2023).

4.2. LA-ICPMS analyses

U-Pb dating of the two samples (LP04, CA06) from the western border of the Principal Cordillera at 32-33° S was conducted at GEMOC. The handpicked zircon grains were bulk-mounted on double-sided adhesive tape and encapsulated in 1-inch epoxy resin pucks. These mounts were polished to expose the zircon interiors, achieving a final surface finish of 0.25 µm. Cathodoluminescence (CL) imaging was conducted using a Zeiss EVO MA15 Scanning Electron Microscope to reveal internal structures and zoning patterns of the zircon grains. These grains were uncolored or pinkish and, ranging in size from 100 to 300 µm with an average of 150 µm for sample CA06. For sample LP04, zircon grains were uncolored to pale orange with a sample size varying from 70 to 350 µm, with 150 µm as average. U-Pb dating was performed using a Photon Machines Excite 193nm excimer laser system equipped with a HelEx II ablation chamber, coupled to an Agilent 7700x ICP-MS. A laser spot diameter of 40 µm was employed. The internal calibration reference material was zircon GJ-1 (Jackson et al., 2004). Primary reference materials, including 91500 (Wiedenbeck et al., 1995), Mud Tank (MT; Black and Gulson, 1978; Gain et al., 2019), and Temora-2 (TEM; Black et al., 2004) zircons, were used to monitor instrument accuracy during the analyses (Supplementary Table 1).

Data reduction was performed using the Glitter® software (Griffin, 2008), and common Pb corrections were applied using ComPbCorr (Anderson, 2002), except if ComPbCorr assumed there was no need for common Pb correction. Age calculations and visualizations, including Concordia diagrams and frequency histograms, were generated using the Isoplot software (Ludwig, 2001, updated). The herewith obtained age clusters were taken directly from the histogram data output. Weighted mean ages were calculated, corrected for common Pb if assumed to be necessary, and interpreted within 95% confidence limits. Calculated ages of samples LP04 and CA06 are listed in Table 1.

It is important to note that, in the two samples analyzed, LP04 and CA06, the zircon spots identified in the CL images were selected randomly without preference for geochronological data acquisition. However, as most analytical spots targeted zircon cores rather than rims, the obtained ages predominantly represent inherited components rather than younger igneous overgrowths recording the timing of magma emplacement or sediment deposition.

4.3. SHRIMP Analyses

High-resolution U-Pb zircon dating of sample N22024 from the Coastal Cordillera (~34° S) was performed using a SIMS-type SHRIMP IIe/MC at IGc-USP. A total of 120 zircon grains, ranging in size from 80 to 150 µm were bulk-mounted alongside the Temora-2 reference standard, polished, and subsequently imaged using CL with a FEI Quanta 250 Scanning Electron Microscope to reveal zircon internal structures. From the 120 bulk-mounted zircon grains, 34 grains were handpicked based on CL images. Initially, any age differences between the rim and core were looked for, but they were observed to vary within the experimental error. Furthermore, selected zircon grains were analyzed on two different days to check on reproducibility and analytical data stability.

Data acquisition utilized a beam spot size of 30 μm. U-Pb calibration followed the methodology of Williams (1998), using LabVIEW 8.5 and SHRIMP SW v2.1 for data acquisition, SQUID 2.5 for data reduction, and Isoplot (Ludwig, 2001, updated) for generating Concordia diagrams. $^{207}Pb/^{235}U$ ages were calculated in offline mode using: $1000\times(1/0.984485)\times\ln(^{207}Pb/^{235}U+1)$.

Common Pb corrections were applied using the Stacey and Kramers (1975) model, or alternatively, the SQUID software for ^{207}Pb and ^{208}Pb corrections. Correction using ^{207}Pb or ^{208}Pb relies on the premise that the $^{207}Pb/^{206}Pb$, $^{206}Pb/^{238}U$, and $^{208}Pb/^{232}Th$ ages are concordant (Williams, 1998). However, this assumption does not always hold in geochronological studies. Correction using ^{204}Pb is generally more reliable, although LA-ICP-MS analyses are affected by interference from ^{204}Hg, as Hg is present in the He and Ar carrier gases. In contrast, SHRIMP analyses are free from ^{204}Hg interference, yet contamination by modern ^{204}Pb may occur, particularly in metamict zircon. In sample N2204, the zircon crystals are not metamict, as demonstrated by the CL images, and surface common Pb was effectively removed by rastering prior to analysis. Therefore, common ^{204}Pb correction was adopted for data reduction in the SHRIMP analyses. The reference material Temora-2 (416.78±0.33 Ma; Black et al., 2004) was used for U-Pb calibration (Supplementary Table 2), while Z6266 (903 ppm U) served to validate measured U concentrations. Analytical uncertainties are reported at the 1σ level (%). For further details on analytical procedures, the reader is referred to Sato et al. (2014). Calculated ages of sample N2204 are listed in Table 2.

5. U-Pb Geochronology

5.1 Crystalline tuff at 32°29' S

Zircon grains from the crystalline tuff LP04 stratigraphically belonging to the Lo Valle Formation (Fig. 2) are elongated with euhedral or subrounded grain rims. They show mainly oscillatory zoning, but some grains have complex textures and xenocrystic cores are frequent (Fig. 4). 46 of the analyzed zircon grains from a total of 58 have calculated $^{206}Pb/^{238}U$ ages in the range 305-339 Ma; of these, 34 gave a weighted mean of about 322±1 Ma (95% confidence) with a MSWD of 0.60 and probability of 0.70, corresponding to the Early Pennsylvanian (Fig. 5A; Table 1A). The age distribution also includes three inherited Neoproterozoic ages, the oldest of which is approximately 860 Ma, alongside one Early Ordovician and one late Silurian age components. Additionally, three Permian ages were identified, as well as five ages younger than 200 Ma, comprising three Early Cretaceous and one Late Cretaceous; the latter represents the estimated maximum age of the crystalline tuff formation (Jackson-Gain, 2023), which is still too old to be assigned to the stratigraphic age of the Lo Valle Formation. The youngest age of 9.9 Ma (Upper Miocene) is interpreted as a probable artifact resulting from laboratory contamination, as it is stratigraphically inconsistent (Jackson-Gain, 2023).

5.2 Miocene granodiorite at 32°42' S

The zircon grains from the granodiorite sample CA06, located in the Campos de Ahumada sector (Fig. 2), are predominantly euhedral crystals or fragments, exhibiting both elongated and stubby morphologies. A few grains are rounded. Most of these crystals display diffuse or complex core textures, surrounded by oscillatory-zoned rims (Fig. 6). Of 77 analyzed zircon spots, the youngest cluster of five concordant zircon ages yields a weighted mean Early Miocene age of 23±1 Ma (Jackson-Gain, 2023). This result is interpreted as the most likely crystallization age of the granodiorite in the Campos de Ahumada sector (Jackson-Gain, 2023). A total of 48 grains (~62%) of the remaining zircon grains yield Carboniferous to early Permian ages (Fig. 5B; Table 1B). Of these, 24 have a weighted mean age of about 309±1 Ma (95% confidence) with an MSWD of 1.14 and a probability of 0.70, corresponding to Middle Pennsylvanian. A secondary age cluster, defined by 18 zircon grains with a weighted mean age of ca. 292 Ma, may reflect the influence of Pb-loss; however, definitive evidence for such a disturbance is lacking. These ages exhibit a continuous distribution ranging from ca. 323 to 285 Ma. Collectively, these two primary inherited populations bracket a temporal range that corresponds to the late Carboniferous-early Permian (Gondwanan orogenic cycle). In addition, there is a minor Mississippian peak (n=6) in the age distribution, and single older inherited ages were identified as Middle Devonian (n=1), middle Silurian (n=1), Middle Ordovician (n=1), and middle Cambrian (n=1) with the oldest at ca. 958 Ma (Neoproterozoic; n=2).

5.3 Coastal Cordillera at 34°17' S

Zircon grains from diorite sample N2204 from the Coastal Cordillera (Fig. 3) exhibit textures typical of magmatic origin, including prismatic morphology and well-defined oscillatory zoning patterns. Some grains contain darker-colored cores; however, $^{206}Pb/^{238}U$ ages from these cores are indistinguishable from those of grains lacking such features, indicating no evidence for xenocrystic inheritance (see selected analyses 1.1, 5.1, 17.2, and 30.2 in Fig. 7 and Table 1). 34 zircon grains separated from the weakly foliated hornblende-biotite diorite yielded a concordia age of 299.2±1.6 Ma (2σ) with an MSWD of 0.93 (Fig. 5C: Table 2). The concordia age plot was used in this case because no inheritance was detected; therefore, the ages uncorrected for common Pb are concentrated in a limited section of the concordia line.

This ca. 299.7 age, which coincides with the Carboniferous-Permian boundary, was also indicated by earlier published studies from this zone (e.g., Gana and Tosdal, 1996; Deckart et al., 2014; Webb and Klepeis, 2019; Jorquera et al., 2023; Velásquez et al., 2024). Therefore, it can be considered as a representative age of the paleo-western Gondwana margin.

6. Discussion

6.1. New ages and the origin of inherited zircons

The zircon U-Pb spectra from samples LP04 and CA06 from the western border of the Principal Cordillera show a dominant late Carboniferous (Pennsylvanian) to early Permian (Cisuralian) inherited signature, accounting for ~60% and 62% of the grain separates, respectively. Given that the stratigraphic and emplacement ages of these two units are significantly younger (Late Cretaceous and Miocene, respectively), the prevalence of these Paleozoic ages indicates that the majority of the analyzed grains are most probably inherited from an unexposed crustal source. The arguments are discussed below for each sample.

Source of zircons in granodiorite CA06

The incorporation of these zircons, either reworked or via partial melting of a Paleozoic basement protolith, enabled the younger granodiorite, as in a possible scenario of sample CA06, to retain a geochronological fingerprint of the Paleozoic basement. As resistant xenocrysts, they survived magmatic transport and provide evidence for the contribution of older, deep-crustal material to Miocene arc magmatism.

The Pocuro Fault system may have facilitated magma ascent and interaction with zircon-bearing Paleozoic crust. This fault system is interpreted as the northern extension of the deep-seated West Andean Thrust (Armijo et al., 2010; Ammirati et al., 2022; Estay et al., 2023), which has accommodated both extensional and compressional regimes since at least the Eocene (Charrier et al., 2005; Jackson-Gain, 2023). This structural discontinuity not only marks the western limit of the Principal Cordillera uplift but also represents the hypothesized western boundary of the Chilenia block (Chernicoff and Zappettini, 2004; Ramos, 2008) or, as more recently used, of the Grenvillian basement (MARA block; Rapela et al., 2016). The significant Carboniferous inheritance observed here suggests that pre-existing fault systems acted as primary conduits for the upward magmatic transport and its possible interaction with Paleozoic unexposed crustal material. This interpretation is further supported by regional evidence at 31°30’ S, where Sigoña et al. (2015) reported granitic enclaves (319±2 Ma) within mafic dikes intruding the Choapa Metamorphic Complex (Willner et al., 2008; Charrier et al., 2024), likewise noticed at around 29°S as indicated by Álvarez et al. (2011). In addition to the local and regional implications of a fault system, it is necessary here to point out that the Miocene granodiorite (CA06) has a strong peraluminous character (Jackson-Gain, 2023), which has been described as highly prone to contain inherited zircons (Tangeman and Mukasa, 1996). Inherited zircons in peraluminous magmas are, however, commonly interpreted as having been derived from the magma source itself rather than being incorporated from rocks encountered during magma ascent (Bea et al., 2021). Thus, the zircon data establish the presence of a Carboniferous-bearing deeper basement component, but cannot distinguish whether this component was incorporated during magma ascent (no assimilation features were observed in the petrographic observations) or was already part of the magma source. Such findings support the existence of a Paleozoic subduction-accretion system and associated intrusive arc magmatism along the paleo-western Gondwana margin (Godoy and Charrier, 1991; Willner, 2005; Willner et al., 2008).

Source of zircons in crystalline tuff LP04

In the case of the Late Cretaceous crystalline tuff (LP04), if the unit formed in-situ, a deep-seated, structurally controlled magma ascent mechanism could account for the observed distribution of inherited zircon ages. However, it remains uncertain whether the inherited zircons represent reworked or recycled crustal material incorporated into the magma. Alternatively, if these zircons are of detrital origin their provenance could be linked to Paleozoic source regions in the Western Sierras Pampeanas or Frontal Cordillera of Argentina (Dahlquist et al., 2021) or the northern Frontal Cordillera of Chile (Maksaev et al., 2014). LP04 is a crystalline tuff containing lithic fragments; however, these fragments were excluded during sample preparation, precluding a direct assessment of their potential contribution to the zircon population. In the northern Frontal Cordillera of Chile, Mesoproterozoic (Grenvillian)-Carboniferous zircon age populations have been identified in detrital zircon suits from late Paleozoic metamorphic complexes between 27° and 29° S, which have been interpreted as components of the Gondwana accretionary prism (Álvarez et al., 2011). Thus, the inherited zircon population in LP04 may reflect either incorporation of pre-existing crustal material during magma generation and ascent or sedimentary recycling from Paleozoic source regions.

Mpodozis and Kay (1992) proposed that a Chilenia component (Grenvillian basement) is reflected in the geochemical signatures of the late Paleozoic to Triassic felsic volcanic and plutonic rocks of the Choiyoi Igneous Province, while xenoliths within the early Permian Elqui-Limarí Batholith have been interpreted as fragments of the Chilenia sialic basement (Ribba et al., 1988). In contrast, U-Pb zircon ages reported by Maksaev et al. (2014) for latest early Carboniferous to middle Permian granitoids and volcanic rocks (~29° S) do not show a significant, if any, Grenvillian basement-derived zircon components. With respect to the data presented by Maksaev et al. (2014), we argue that structurally controlled magma ascent provides a more plausible explanation for the occurrence of inherited zircons in younger lithologies. Deep crustal fault zones may have acted as conduits, allowing ascending magmas to interact with otherwise unexposed Gondwanan basement and incorporate inherited zircons. This interpretation is consistent with our hypothesis that the Carboniferous zircon populations reflect localized crustal inheritance associated with major structural corridors, rather than widespread detrital recycling from regional Paleozoic or even Proterozoic basement sources.

In samples from the Principal Cordillera (32-33° S), the absence of Mesoproterozoic (Grenvillian) zircon ages is significant, as it contrasts with the basement signatures typically observed in adjacent Andean segments. While the Grenvillian basement is physically well exposed in the Western Sierras Pampeanas in Argentina, its presence beneath the Chilean Principal Cordillera is mainly inferred from geochemical interpretations and/or inheritance in Cretaceous and Neogene magmatic units. Such inheritance and additional geochemical trace element ratios and isotope data have been used extensively to argue for the presence of the Cuyania block (Grenvillian age) as primary basement components at this latitude (e.g., Zentilli et al., 2001; Large et al., 2024). In the Principal Cordillera of Central Chile (33° S), the evidence for Proterozoic basement remains isolated; for instance, while a single Mesoproterozoic upper intercept age was reported for the quartz-monzonite porphyry at the Río Blanco-Los Bronces deposit, the majority of other upper intercept ages of porphyries in the area cluster in the late Paleozoic (Deckart et al., 2005). The near-total lack of Grenvillian ages in the studied samples (e.g., Boyce et al., 2020; Payacán et al., 2024; Gerding et al., 2026) suggests that the

Chilenia block (Grenvillian) does not constitute the immediate basement, at least not at the crustal depths sampled by the parental magmas during their ascent. Instead, the data imply a lithospheric architecture dominated by Carboniferous-early Permian lithologies. This interpretation aligns with recent findings by Dahlquist et al. (2025) and is further corroborated by the geochronological results from the Late Cretaceous and Miocene units presented in this study. Besides, it suggests that the Gondwanan Carboniferous-early Permian margin maintains, most probably, lateral continuity at depth either from the Coastal Cordillera (31°30' S) to the Western Sierras Pampeanas in Argentina or from the northern part of the Chilean Frontal Cordillera into the herewith studied zone at 32-34° S, suggesting a potentially continuous Paleozoic basement component at depth. This interpretation, however, remains tentative given the limited dataset.

6.2. Implications for the tectonomagmatic configuration and the extent of the Gondwana Cycle

The integration of these new age data with previously published geochemical and isotopic records suggests a major shift in the regional tectonomagmatic regime and helps delineate the lateral extent of the Paleozoic magmatic arc.

In the Coastal Cordillera at 34° S, the Pailimo Unit (N2204), part of the Carboniferous-Permian Intrusive Unit within the paired metamorphic belt of North-Central Chile (e.g., Hervé et al., 1987, 1988; Hervé, 1988; Willner et al., 2005, 2008), yielded a robust late Carboniferous (Pennsylvanian) age of 299.7±1.2 Ma. Unlike the samples from the western border of the Principal Cordillera, the Pailimo Unit, characterized by having a metaluminous character, shows no evidence of older inherited components, representing a primary magmatic expression of the Carboniferous Intrusive Complex. This age is consistent with the magmatic belt extending from 33° S to 40° S, as indicated by the additional eight late Carboniferous-early Permian Coastal Batholith intrusive rock samples analyzed by Deckart et al. (2014). Collectively, these samples show a notable absence of Mesoproterozoic inherited zircon, supporting the interpretation of a predominantly Paleozoic crustal component along this segment of the magmatic belt.

The clear identification of this primary arc segment at 34° S, when contrasted with the inherited signatures identified at 32-33° S (Section 6.1), suggests that Carboniferous magmatism in central Chile forms part of a contiguous magmatic domain at depth. And moreover, rather than reflecting discrete or exotic contributions from the Chilenia block (characterized by Grenvillian ages), the data indicate a marked, late Paleozoic arc expression that remains preserved within the unexposed crust. Therefore, it is proposed that the Paleozoic basement at 32-33° S was intermittently entrained during younger magmatic episodes, particularly where deep-seated structural discontinuities facilitated the ascent of mantle-derived melts and their subsequent assimilation of the crustal lithology. On the other hand, a detrital origin for the predominantly late Carboniferous zircon population appears unlikely. If these zircons were derived from regional detrital sources, comparable Carboniferous age populations would be expected across diachronous lithological units throughout the study area. Instead, inherited late Carboniferous zircons are restricted to the lithologies presented here (Late Cretaceous and Miocene), whereas comparable units elsewhere do not display this particular age signature (e.g., Boyce et al., 2020; Payacán et al., 2024; Gerding et al., 2026). Furthermore, the limited number of Grenvillian-age zircons neither supports the presence of a significant Chilenia-derived basement beneath this segment of the Principal Cordillera. This interpretation is consistent with the geochronological data of Maksaev et al. (2014) on intrusives from ~29° S, Boyce et al. (2012) and Gerding et al. (2026) on Cretaceous to Late Cretaceous igneous rocks at 32-33° S, and Payacán et al. (2024) on a Miocene intrusive (33°40' S), which likewise do not indicate the presence of a substantial Grenvillian basement component.

On this basis, we propose that the Pocuro Fault system may have acted as a localized structural conduit, particularly for the Miocene magmatism, facilitating magma ascent and interaction with an otherwise unexposed Carboniferous-bearing crustal component at 32-33° S. The resulting inherited zircon signature may therefore reflect localized interaction with, or partial melting of, Paleozoic crust rather than widespread incorporation of Grenvillian zircons from a Chilenia-related basement. This interpretation provides a plausible mechanism linking the Carboniferous inherited zircon populations observed at 32-33° S with the broader Carboniferous-Permian magmatic system documented north (21-29° S) and farther south along the Chilean Coastal Cordillera (33-40° S).

These findings highlight the need for integrated high-resolution geochronology and regional isotopic mapping (e.g., Lu-Hf and $\delta^{18}O$ in zircon) to fully delineate the deep-crustal architecture and characterize the lithospheric boundaries of this segment of the Andes. Furthermore, there is a critical need to interpret these

Carboniferous-late Permian lithologic units within the broader context of the presence or absence of the Paleozoic accretionary prism along the western Gondwana margin. Such a synthesis is essential to understanding the transition from a late Paleozoic subduction-accretion system to the modern Andean-type margin.

7. Conclusions

The geochronological data presented in this study provide new insights into the crustal architecture and tectonomagmatic evolution of the central Chilean Andes. Based on the U-Pb zircon age spectra from the western border of the Principal Cordillera (32-33° S) and the Coastal Cordillera (34° S), the following conclusions are drawn:

- **Evidence of a Paleozoic basement**: The high frequency of inherited zircon ages (60-62%) in Late Cretaceous and Miocene units at 32-33° S suggests the presence of a late Carboniferous to early Permian lower crustal basement. If inherited zircon minerals are of reworked or recycled nature stays for debate. Regarding the Gondwanan magmatic arc, it is suggested that it represents a laterally continuous lithospheric framework extending at depth from the Coastal Cordillera of Chile through the Chilean Frontal Cordillera to the Western Sierras Pampeanas of Argentina.
- **Structural control on magmatic inheritance:** The spatial association of these inherited signatures with the Pocuro Fault system suggests that this long-lived, deep-seated crustal discontinuity, interpreted as the northern extension of the West Andean Thrust, acted as a primary conduit. These pre-existing structurally

weakened zones facilitated the upward transport of a Paleozoic zircon-bearing magma and may also have promoted the interaction with Paleozoic unexposed crustal material. Still, this suggestion is based on only a few samples, therefore, further research has to be conducted.

- **Absence of exotic blocks signatures:** The near-total absence of Mesoproterozoic (Grenvillian) ages in samples from the western border of the Principal Cordillera suggests that the Chilenia block (Grenvillian) does not form the immediate basement in this Andean segment. This contrasts with observations in the Western Sierra Pampeanas in Argentina, implying significant latitudinal or depth-dependent variations in the lithospheric architecture of the Chilean margin.
- **Primary arc expression at 34° S:** The 299.2±1.6 Ma age obtained from the Pailimo Unit at 34° S represents a primary expression of the Carboniferous-Permian magmatic arc. Unlike the inherited signatures of the western border of the Principal Cordillera (32-33° S), the lack of inheritance in this unit aligns with the broader magmatic belt of south-central Chile (33-40° S; Deckart et al., 2014), where Proterozoic signatures are similarly absent.

In conclusion, interpretation of the Carboniferous-early Permian magmatic arc is currently limited to only three samples. Additional integrated isotope-geochemical studies are essential to constrain its extent, geodynamic significance, and implications for crustal architecture during Gondwana assembly.

Acknowledgements

The research work was supported by Fondecyt N°1200871 (L. Pinto) regarding samples LP04 and CA06: U-Pb analyses of these 2 samples were performed by Yoann Gréau at MQ GeoAnalytical, Department of Earth and Environmental Sciences, Macquarie University, Sydney, Australia. N2204 belongs to the Project Exploración N°13220141 (F. Hervé, M. Calderón). We would like to thank J. Vargas (JV Circones y Minerales SpA) for zircon separations. We are grateful to K. Agurto for preparing figures 1 and 3. The authors acknowledge the constructive comments and valuable suggestions of two anonymous reviewers and C. Creixell, which significantly helped improve the quality and clarity of the manuscript. This paper is dedicated to Prof. Francisco Hervé in recognition of his outstanding contributions over several decades to the study of the western Gondwana margin.

References

Álvarez, J.; Mpodozis, C.; Arriagada, C.; Astini, R.; Morata, D.; Salazar, E., Valencia, V.A.; Vervoort, J.D. 2011. Detrital zircons from late Paleozoic accretionary complexes in north-central Chile (28-32°S): Possible fingerprints of the Chilenia terrane. Journal of South American Earth Sciences 32, 460-476. doi:10.1016/j.jsames.2011.06.002.

Ammirati, J.-B.; Villaseñor, A.; Chevrot, S.; Easton, G.; Lehujeur, M.; Ruiz, S.; Flores, M.C. 2022. Automated Earthquake Detection and Local Travel Time Tomography in the South-Central Andes (32–35°S): Implications for Regional Tectonics. Journal of Geophysical Research: Solid Earth 127: e2022JB024097. https://doi.org/10.1029/2022JB024097.

Anderson, T. 2002. Correction of common lead in U-Pb analyses that do not report 204Pb. Chemical Geology 192 (1-2): 59-79.

Armijo, R.; Rauld, R.; Thiele, R.; Vargas, G.; Campos, J.; Lacassin, R.; Kausel, E. 2010. The West Andean thrust, the San Ramon fault, and the seismic hazard for Santiago, Chile. Tectonics 29(2): TC2007. https://doi.org/10.1029/2008TC002427.

Ariza, J.P.; Florencia, L.B.; Sánchez, M.A.; Christiansen, R.; Pérez Lujan, S.B.; Vujovich, G.I.; Martínez, P. 2018. Structural setting of the Chanic orogen (Upper Devonian) at central-western Argentina from remote sensing and aeromagnetic data. Implications in the evolution of the proto-Pacific margin of Gondwana. Journal of South American Earth Sciences 88: 352-366.

Bea, F.; Morales, I.; Molina, J. F.; Montero, P.; Cambeses, A. 2021. Zircon stability grids in crustal partial melts: implications for zircon inheritance. Contributions to Mineralogy and Petrology, 176(3): 18.

Black, L.P.; Kamo, S.L.; Allen, C.M.; Davis, D.W.; Aleinikoff, J.N.; Valley, J.W.; Mundil, R.; Campbell, I.H.; Korsch, R.J.; Williams, I.S.; Foudoulis, C. 2004. Improved 206Pb/238U microprobe geochronology by the monitoring of a trace-element-related matrix effect; SHRIMP, ID–TIMS, ELA–ICP–MS and oxygen isotope documentation for a series of zircon standards. Chemical Geology 205 (1-2): 115-140.

Black, L.P.; Gulson, B.L. 1978. The age of the Mud Tank Carbonatite, Strangways Range, Northern Territory. BMR Journal of Australian Geology and Geophysics 3: 227-232.

Boyce, D.; Charrier, R.; Farías, M. 2020. The First Andean Compressive Tectonic Phase: Sedimentologic and Structural Analyses of Mid-Cretaceous Deposits in the Coastal Cordillera, Central Chile (32°50'S). Tectonics 39: e2019TC005825.

Charrier, R.; Bustamante, M.; Comte, D.; Elgueta, S.; Flynn, J.J.; Iturra, N.; Muñoz, N.; Pardo, M.; Thiele, R.; Wyss, A. 2005. The Abanico extensional basin: Regional extension, chronology of tectonic inversion and relation to shallow seismic activity and Andean uplift. Neues Jahrbuch für Geologie und Paläontologie - Abhandlungen 236: 43–77. https://doi.org/10.1127/njgpa/236/2005/43.

Charrier, R.; Hervé, F.; Muñoz-Gomez, M.; Fanning, C.M.; Moisan, P.; Rebolledo, S.; Rojas del Castillo, M. 2024. The Early Carboniferous age of the Arrayán Formation in the Choapa Accretionary Complex: Implications for its fossil floral content, tectonic setting and evolution of the southwestern Gondwana margin (north-central Chile). Journal of South American Earth Sciences 148. 105161. https://doi.org/10.1016/j.jsames.2024.105161.Cawood, P.A. 2005. Terra Australis Orogen: Rodinia breakup and development of the Pacific and Iapetus margins of Gondwana during the Neoproterozoic and Paleozoic. Earth-Science Reviews 69: 249-279. doi:10.1016/j.earscirev.2004.09.001

Cawood, P.A.; Buchan, C. 2007. Linking accretionary orogenesis with supercontinent assembly. Earth-Science Reviews 82 (3-4): 217-256.

Chernicoff, C.; Zappettini, E. 2004. Geophysical evidence for terrane boundaries in southcentral Argentina. Gondwana Research 7: 1105–1116.

Cohen, K.M.; Finney, S.C.; Gibbard, P.L.; Fan, J.-X. 2013 (updated). The ICS International Chronostratigraphic Chart. Episodes 36: 199-204.

Creixell, Ch.; Sepúlveda, F.; Alvarez, J.; Vásquez, P.; Velásquez, R. 2021. The Carboniferous onset of subduction at SW Gondwana revisited: Sedimentation and deformation processes along the late Paleozoic forearc of north Chile (21◦–33◦ S). Journal of South American Earth Sciences 107: 103149.

Creixell, Ch.; Díaz-Alvarado, J.; Alvarez, J.; Rodríguez, C.; Velásquez, R.; Oliveros, V. 2025. Episodic magmatism and segmentation of the Gondwanan arc in Chile (21–38◦S): Insights into Carboniferous to early Permian subduction processes and deformation. Journal of South American Earth Sciences 156: 105421.

Dahlquist, J.A.; Morales Cámera, M.M.; Alasino, P.H.; Pankhurst, R.J.; Basei, M.A.S.; Rapela, C.W.; Moreno, J.A.; Baldo, E.G.; Galindo, C. 2021. A review of devonian–carboniferous magmatism in the central region of Argentina, pre-andean margin of SW Gondwana. Earth-Science Reviews 221: 103781. https://doi.org/10.1016/j.earscirev.2021.103781.

Dahlquist, J.A.; Ramacciotti, C.D.; Morales Cámera, M.M.; Basei, M.A.S.; Santos da Cruz, G.; Gonzalez, G. A. 2025. The 40th anniversary of the Chilenia terrane: Where is its Grenville-age basement? Journal of South American Earth Sciences 164, 105638. https://doi.org/10.1016/j.jsames.2025.105638.

Davis, J.S.; Roeske, S.M.; Mc Clelland, W.C.; Kay, S.M. 2000. Mafic and ultramafic crustal fragments of the southwestern Precordillera terrane and their bearing on tectonic models of the early Paleozoic in western Argentina. Geology 28 (2): 171–174.

Deckart, K.; Clark, A.H.; Aguilar, C.; Vargas, R. 2005. Magmatic and hydrothermal chronology of the supergiant Río Blanco Porphyry Copper Deposit, Central Chile: Implications of an integrated U/Pb and 40Ar/39Ar database. Economic Geology 100 (5): 905-934.

Deckart, K.; Hervé, F.; Fanning, M.; Ramírez, V.; Calderón, M.; Godoy, E. 2014. U-Pb geochronology and Hf-O isotopes of zircons from the pennsylvanian coastal batholith, South-Central Chile. Andean Geology 41 (1): 49e82.

Del Rey, A.; Deckart, K.; Arriagada, C.; Martínez, F. 2016. Resolving the paradigm of the late Paleozoic-Triassic Chilean magmatism: Isotopic approach. Gondwana Research 37: 172-181.

Del Rey, A.; Deckart, K.; Planavsky, N.; Arriagada, C.; Martínez, F. 2019. Tectonic evolution of the southwestern margin of Pangea and its global implications: Evidence from the mid Permian-Triassic magmatism along the Chilean-Argentine border. Gondwana Research 76: 303-321.

De la Cruz, R.; Suárez, M. 2006. Geología del área Puerto Guadal-Puerto Sánchez, Región Aisén del General Carlos Ibáñez del Campo, Escala 1:100.000, Carta Geológica de Chile. In Serie Geología Básica 95: 58 pp. Servicio Nacional de Geología y Minería, Santiago, Chile.

Estay, J.; Pinto, L.; Easton, G.; De Pascale, G.P.; Troncoso, M.; Carretier, S.; Forman, S.L. 2023. Active thrust tectonics along the western slope of the Central Andes southernmost Pampean flat-slab segment (33°S, Chile): The Cariño Botado fault system. Geomorphology 437: 108801. https://doi.org/10.1016/j.geomorph.2023.108801

Gerding V.; Muñoz-Gómez, M.; Encinas, A.; Quiñones, S.; Castro D.; Charrier, R; Valencia, V.; Le Roux, P. 2026. Tectono-magmatic transition from compression to extension along the central Chilean margin (~33◦S) during the Late Cretaceous: Insights from volcanic arc units. Lithos 542-543: 108723. https://doi.org/10.1016/j.lithos.2026.108723.

Gain, S.E.M.; Gréau, Y.; Henry, H.; Belousova, E.; Dainis, I.; Griffin, W.L.; O'Reilly, S.Y. 2019. Mud Tank Zircon: Long-term evaluation of a reference material for U-Pb dating, Hf-isotope analysis and trace element analysis. Geostandards and Geoanalytical Research 43: 339-354. https://doi.org/10.1111/ggr.12265.

Gana, P.; Wall, R.; Gutierrez, A. 1996. Mapa Geológico del Área, Valparaíso – Curacaví, regiones de Valparaíso y Metropolitana. Servicio Nacional de Geología y Minería, Mapas Geológicos, No. 1, escala 1:100.000.

Gana, P.; Tosdal, R. 1996. Geocronología U-Pb y K-Ar en intrusivos del Paleozoico y Mesozoico de la Cordillera de la Costa, Región de Valparaíso, Chile. Revista Geológica de Chile 23 (2): 151-164.

Godoy, E.; Charrier, R. 1991. Antecedentes Mineralógicos para el origen de las metabasitas y metacherts del Complejo Metamórfico del Choapa (Región Coquimbo, Chile): Un prisma de acreción Paleozoico inferior. In VI Congreso Geológico Chileno, Resúmenes Extendidos: 410-414. Viña del Mar.

Griffin W.L. (2008). GLITTER: data reduction software for laser ablation ICP-MS. Laser Ablation ICP-MS in the Earth Sciences: Current practices and outstanding issues. Mineralogical Association of Canada 40: 308-311.

Heredia, N.; García-Sansegundo, J.; Gallastegui, G.; Farias, P.; Giacosa, R.; Hongn, F.; Tubía, J.M.; Alonso, J.L.; Busquets, P.; Charrier, R.; Clariana, P.: Colombo, F.; Cuesta, A.; Gallastegui, J.; Giambiagi, L.; González-Menéndez, L.; Limarino, C.O.; Martín-González, F.; Pedreira, D.; Quintana, L.; Rodríguez-Fernández, L.R.; Rubio-Ordóñez, A.; Seggiaro, R.E.; Serra-Varela, S.; Spalletti, L.; Cardó, R.; Ramos, V.A. 2017. The Pre-Andean phases of construction of the Southern Andes basement in Neoproterozoic-Paleozoic times. In: Folguera, A.; Contreras Reyes, E.; Heredia, N.; Encinas, A.; Iannelli, S.; Oliveros, V.; Dávila, F.; Collo, G.; Giambiagi, L.; Maksymowicz, A.; Iglesia Llanos, P.; Turienzo, M.; Naipauer, M.; Orts, D.M.; Litvak, V.; Alvarez, O.; Arriagada, C. (Eds.), The Evolution of the Chilean Argentinean Andes. Springer, 133-153. Earth System Sciences.

Heredia, N.; García-Sansegundo, J.; Gallastegui, G.; Farias, P.; Giacosa, R.; Alonso, J.L.; Busquets, P.; Charrier, R.; Clariana, P.; Colombo, F.; Cuesta, A.; Gallastegui, J.; Giambiagi, L.; González-Menéndez, L.; Limarino, C.O.; Martín-Gonzalez, F.; Pedreira, D.; Quintana, L.; Rodríguez-Fernández, L.R.; Rubio-Ordoñez, A.; Seggiaro, R.; Serra-Varela, S.; Spalletti, L.; Cardo, R.; Ramos, V.A. 2016. Evolución Geodinámica de los Andes de Argentina, Chile y la Península Antártica durante el Neoproterozoico superior y el Paleozoico. Trabajos de Geología 36, Universidad de Oviedo: 237-278.

Heredia, N.; García-Sansegundo, J.; Gallestegui, G.; Farias, P.; Giacosa, R.E.; Giambiago, L.B.; Busquets, P.; Colombo, F.; Charrier, R.; Cuesta, A.; Rubio-Ordoñez, A.; Ramos., V.A. 2018. Review of the geodynamic evolution of the

SW margin of Gondwana preserved in the Central Andes of Argentina and Chile (28-38 S latitude). Journal of South American Earth Sciences 87: 87-94.

Hervé, F. 1988. Late Paleozoic Subduction and Accretion in Southern Chile. Episodes 11(3): 183-188.

Hervé, F.; Godoy, E.; Parada, M.; Ramos, V.; Rapela, C.; Mpodozis, C.; Davidson, J. 1987. A general view on the Chilean-Argentine Andes, with emphasis on their early history. In: Monger, J.W.H. & Francheteau (eds.) 1987: Circum-Pacific Orogenic Belts and Evolution of the Pacific Ocean Basin Geodynamics Series 18: 97–113.

Hervé, F.; Munizaga, F.; Parada, M.A.; Brook, M.; Pankhurst, R.J.; Snelling, N.J., Drake, R. 1988. Granitoids of the coast range of central Chile: geochronology and geologic setting. Journal of South American Earth Sciences 1(2): 185–194. https://doi.org/10.1016/0895-9811(88)90036-3.

Hervé, F.; Faundez, V.; Calderón, M.; Massonne, H.-J.; Willner, A.P. 2007. Metamorphic and plutonic basement complexes. In: Moreno, T. & Gibbons, W. (eds.) 2007: The Geology of Chile. The Geological Society, London. Chapter 2: 21 p. Society, London.

Hervé, F.; Fanning, C.M.; Calderón, M.; Mpodozis, C. 2014. Early Permian to late Triassic batholiths of the Chilean frontal cordillera (28° -31° S): SHRIMP U-Pb zircon ages and Lu-Hf and O isotope systematics. Lithos 184: 436-446.

Hervé, F.; Calderón, M.; Fanning, C.M.; Pankhurst, R.J.; Fuentes, F.; Rapela, C.W.; Correa, J.; Quezada, P.; Marambio, C. 2016. Devonian magmatism in the accretionary complex of southern Chile. Journal of Geological Society London 173: 587–602. https://doi.org/10.1144/jgs2015-163.

Hyppolito, T.; Juliani, C.; García-Casco, A.; Meira, V.T.; Bustamante, A.; Hervé, F. 2014. The nature of the Palaeozoic oceanic basin at the southwestern margin of Gondwana and implications for the origin of the Chilenia terrane (Pichilemu region, central Chile). International Geology Review 56: 1097-1121.

Jackson, S.E.; Pearson, N.J.; Griffin, W.L.; Belousova, E.A. 2004. The application of laser ablation-inductively coupled plasma-mass spectrometry to in situ U–Pb zircon geochronology. Chemical Geology 211 (1-2): 47-69.

Jackson-Gain, A. 2023. Análisis cronoestratigráfico y geoquímico de las unidades mesozoicas y cenozoicas en el entorno del borde occidental de la Cordillera Principal en Chile Central (32-33°S). Magister (Unpublished), Universidad de Chile: 209 p.

Jorquera, R.; Domagala, J.; Villa, V., Astudillo, N. 2023. Geología del área Pichibelco-Cauquenes, región del Maule. Servicio Nacional de Geología y Minería, Carta Geológica de Chile, Serie Geología Básica 214: 151 p., 1 mapa escala 1:100.000. Santiago.

Large, S.J.E.; Nathwani, C.L.; Wilkinson, J.J.; Knott, T.R.; Tapster S.R.; Buret, Y. 2024. Tectonic and Crustal Processes Drive Mult-Million Year Arc Magma Evolution Leading up to Porphyry Copper Deposit Formation in Central Chile.

Ludwig, K.R. 2001 updated. Isoplot/Ex version 2.49: A geochronology toolkit for Microsoft Excel. Berkeley Geochronology Center Special Publication: 55.

Maksaev, V.; Munizaga, F.; Tassinari, C. 2014. Timing of the magmatism of the paleo- Pacific border of Gondwana: U–Pb geochronology of Late Paleozoic to Early Mesozoic igneous rocks of the north Chilean Andes between 20° and 31°S. Andean Geology 41: 447–506. http://dx.doi.org/10.5027/andgeoV41n3-a01.

Marcos, P.; Renda, E.M.; González, P.D.; Oriolo, S.; Scivetti, N.; Benedini, L.; Geraldes, M.; Gregori, D.; Yoya, M.B.; Bahía, M. 2023. Devonian to Early Carboniferous Retreating–Advancing Subduction Switch in the Northwestern Patagonia Accretionary Orogen: U–Pb and Lu–Hf Isotopic Insights. Tectonics 42(11): 1–22. https://doi.org/10.1029/2022TC007533.

Mella, M.; Quiroz, D. 2023. Granito Svea: Magmatismo devónico-carbonífero en Cordillera de Darwin, Tierra del Fuego, Chile. In XVI Congreso Geológico Chileno, AT1-11. Tectónica del Arco de Scotia, Santiago.

Moreno, J.A.; Dahlquist, J.A.; Morales Cámera, M.M.; Alasino, P. H.; Larrovere, M.A.; Basei, M.A.S.; Galindo, C.; Zandomeni, P. S.; Roche, S. 2020. Geochronology and geochemistry of the tabaquito batholith (frontal cordillera, Argentina): Geodynamic implications and temporal correlations in the SW Gondwana margin: Journal of the Geological Society of London 177: 455–474.

Pankhurst, R.J.; Hole M.J.; Brook, M. 1988. Isotope evidence for the origin of Andean granites. Transaction of the Royal Society of Edinburgh: Earth Sciences 79: 123-133.

Pankhurst, R.J.; Rapela, C.W.; Fanning, C.M.; Márquez, M. 2006. Gondwanide continental collision and the origin of Patagonia. Earth-Science Reviews 76(3-4): 235-257.

Pankhurst, R.J.; Rapela, C.W.; Loske, W.; Marquéz, M.; Fanning, C.M. 2003. Chronological study of the pre-Permian basement rocks of southern Patagonia. Journal of South American Earth Sciences 16: 27–44.

Pankhurst, R.J.; Rapela, C.W. 1998. The proto-Andean margin of Gondwana: an introduction. Geological Society, London, Special Publications 142: 1-9.

Parada, M.A. (1990): Granitoid plutonism in Central Chile and its geodynamic implications: a review. *In*: Mahlburg Kay, S. y Rapela, C. W. (eds.), Plutonism from Antarctica to Alaska. Geological Society of America Special Paper, 241: 51-65.

Payacán, I.; Covarrubias, M.A.; Rodríguez, N.; Tavazzani, L.; Gutiérrez, F.; Roperch, P.; Poblete, F.; Meyer, M. 2024. Diverse intrusion modes during the construction of a high-silica magma reservoir: Evidence from La Obra-Cerro Blanco intrusive suite (central Chile). Geosphere 20(6): 1622-1654.

Ramos, V.A. 1988. Tectonics of the Late Proterozoic – Early Paleozoic: a collisional history of southern South America. Episodes 11: 168-174.

Ramos, V.A.; Cristallini, E.O.; Pérez, D.J. 2002. The Pampean flat-slab of the Central Andes. Journal of South American Earth Sciences 15: 59-78.

Ramos, V.A. 2004. Cuyania, an Exotic Block to Gondwana: Review of a Historical Success and the Present Problems. Gondwana Research 7(4): 1009-1026.

Ramos, V.A.; Folguera, A. 2009. Andean flat-slab subduction through time. In Ancient Orogens and Modern Analogues, Geological Society, London, Special Publication, Murphy, B., Keppie, J.D., Hynes, A.J., 327: 31-54.

Rapela, C.W.; Pankhurst, R.J.; Casquet, C.; Baldo, E.; Galindo, C.; Fanning, C.M.; Dahlquist, J.M. 2010. The Western Sierras Pampeanas: protracted Grenville-age history (1330–1030 Ma) of intra-oceanic arcs, subduction-accretion at continental edge and AMCG intraplate magmatism. Journal of South American Earth Sciences 29: 105–127.

Rapela, C.W.; Hervé, F.; Pankhurst, R.J.; Calderón, M.; Fanning, C.M.; Quezada, P.; Poblete, F.; Palape, C.; Reyes, T. 2021. The Devonian accretionary orogen of the North Patagonian cordillera. Gondwana Research, 96, 1–21. https://doi.org/10.1016/j.gr.2021.04.004.

Renda, E.M.; Marcos, P.; Oriolo, S.; Putlitz, B.; Baumgartner, L.; González P.; Foley, M.L.; Ruiz González, V.; Vizán, H. 2025. Counterclockwise P-T-t path, cyclic crustal anatexis and magmatic tempo in accretionary orogens: A case study in the Devonian arc of Central Patagonia, Argentina. Gondwana Research 141: 310-331. https://doi.org/10.1016/j.gr.2025.02.011.

Rivano, S.; Sepúlveda, P.; Boric, R.; Espiñeira, D. 1993. Hojas Quillota y Portillo, V Región. In: Map 73, scale 1:250,000. Servicio Nacional de Geología y Minería, Carta Geológica de Chile.

Rocher, S.; Alasino, P.H.; Dahlquist, J.A.; Basei, M.A.S. 2024. Permian-Triassic volcanic and plutonic records of the Argentine Frontal Cordillera: A review with new U–P and Hf-isotope zircon data. Journal of South American Earth Sciences, 149: 105181, 0895-9811.

Rossel, K.; Aguilar, G.; Salazar, E.; Martinod, J.; Carretier, S.; Pinto, L., Cabré, A. 2016. Chronology of Chilean Frontal Cordillera building from geochronological, stratigraphic and geomorphological data insights from Miocene intramontane-basin deposits. Basin Research 30(S1): 289-310.

Rossel, P.; Suárez, M.; Morata, D.; de la Cruz, R. 2024. Low-δ18 O in mississippian los leones granite (46° S). Tectonic implications for the understanding of late paleozoic evolution in patagonia. Journal of South American Earth Sciences 148: 105174.

Sato, K.; Gaeta T., C.C.; Stipp B., M.A.; Siga Jr., O.; Takashi O., A.; Dias de Souza, M. 2014. Sensitive High Resolution Ion Microprobe (SHRIMP IIe/MC) of the Institute of Geosciences of the University of São Paulo, Brazil: analytical method and first results. Revista do Instituto de Geociencias – USP, 14 (3): 3-18. Doi:10.5327/Z1519-874X201400030001.

Santos da Cruz, G.; Moreno, J.A.; Dahlquist, J.A.; Morales Cámera, M.M.; Basei, M.A.S.; Zandomeni, P.S. 2024. Contributing to understand how Cordilleran batholiths build from detailed geochronology of the Carboniferous Tabaquito batholith, Frontal Cordillera (Argentina). In: Molina, J.F.; Cambeses, A.; García Casco, A.; Montero, P. (Eds.), F. Bea's Work Celebration, Chemical Geology, 662: 122245.

Sernageomin, 2003. Mapa geológico de Chile: versión digital. Escala 1:1.000.000.

Sigoña, P.; Charrier, R.; Muñoz, M.; Tapia, F.; Farías, M. 2015. Petrología y geocronología de enclaves graníticos del Paleozoico superior en diques mesozoicos en el sector costero del Norte chico (31°30´S), Chile. In XIV Congreso Geológico Chileno, AT1: 546-550. La Serena.

Stacey, J.S.; Kramers, J.D. 1975. Approximation of terrestrial lead isotope evolution by a two-stage model. Earth and Planetary Science Letters 26 (2): 207-221.

Tangeman, J.A.; Mukasa, S.B. 1996. Zircon U-Pb geochronology of plutonic rocks from the Antarctic Peninsula: Confirmation of the presence of unexposed Paleozoic crust. Tectonics 15(6): 1309-1324.

Thomas, H. 1958. Geología de la Cordillera de la Costa entre el valle de La Ligua y la cuesta Barriga. Instituto de Investigaciones Geológicas, Boletín 2: 86 p.

Varela, R.; Basei, M.A.S.; González, P.D.; Sato, A.M.; Naipauer, M.; Campos Nieto, M.; Cingolani, C.A.; Meira, V.T. 2011. Accretion of Grenvillian terranes to the southwestern border of the Río de la Plata craton, western Argentina. International Journal of Earth Sciences 100 (2): 243-272. Doi:10.1007/s00531-010-0614-2.

Vaughan, A.P.M.; Pankhurst, R.J. 2008. Tectonic overview of the West Gondwana margin. Gondwana Research 13: 150-162.

Velásquez, R., Merino, R., Creixell, C., 2024. New U-Pb zircons and Ar-Ar micas ages or the southern coastal batholith of Central Chile in Maule and Biobío regions, Chile. In: Book of Abstracts of the XIII South American Symposium on Isotope Geology, 2024, Búzios. Anais Eletrónicos. Campinas, Galoá, 2024.

Webb, L.; Klepeis, K. 2019. 40Ar/39Ar constraints on the tectonic evolution of the late Paleozoic and early Mesozoic accretionary complex of coastal central Chile. In: Horton, B., Folguera, A. (Eds.), Andean Tectonics. Elsevier, 531–553. https://doi. org/10.1016/B978-0-12-816009-1.00020-4.

Weil, A.B.; Van der Voo, R.; Mac Niocaill, C.; Meert, J.G. 1998. The Proterozoic supercontinent Rodinia: paleomagnetically derived reconstructions for 1100 to 800 Ma. Earth and Planetary Science Letters 154: 13-24.

Wiedenbeck, M.; Allé, P.; Corfu, F.; Griffin, W.L.; Meier, M.; Oberli, F.; von Quadt, A.; Roddick, J.C.; Spiegel, W. 1995. Three natural zircon standards for U-Th-Pb, Lu-Hf, trace element and REE analyses. Geostandards Newsletter 19 (1): 1-23.

Williams, I.S. 1998. U-Th-Pb geochronology by ion microprobe. In Applications of Microanalytical Techniques to Understanding Mineralizing Processes (McKibben, M.A.; Shanks III, W.C.; Ridley, W.I.; editors). Reviews in Economic Geology 7: 1-35.

Willner, A.P.; Thomson, S.N.; Kröner, A.; Wartho, J.-A.; Wijbrans, J.R.; Hervé, F. 2005. Time Markers for the Evolution and Exhumation History of a Late Palaeozoic Paired Metamorphic Belt in North–Central Chile (34°–35°30”S). Journal of Petrology 46: 1835-1858.

Willner, A.P.; Gerdes, A.; Massonne, H.J. 2008. History of crystal growth and recycling at the Pacific convergent margin of South America at latitudes 29◦-36◦S revealed by a U-Pb and Lu-Hf. isotope study of detrital zircon from late Paleozoic accretionary systems. Chemical Geology 253 (3): 114–129.

Zentilli, M.; Pop, N.; Heaman, L.; Boric, R. 2001. Evidence of Proterozoic crust under the Coastal Cordillera of Central Chile: Grenville age xenocrystic zircons in Cretaceous volcanic rocks. *In*: South American Isotope Conference, CD-ROM 642. Chile.

Figure and table captions

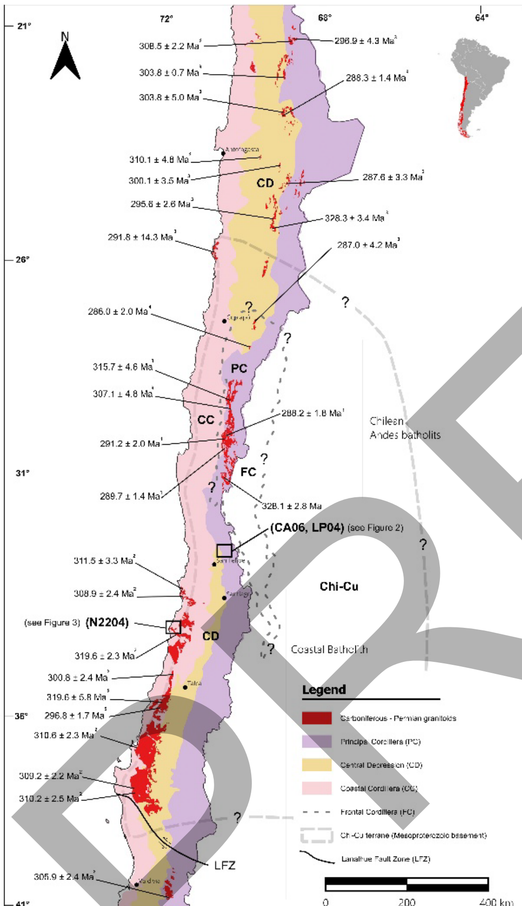

Figure 1

Fig. 1. Geographical distribution of Carboniferous-early Permian intrusive rocks along the Chilean Andes, from 21° S to 41° S. Inferred Chi-Cu terrane (Chilenia-Cuyania) is shown as a grey segmented line, approximate limits defined according to Ramos (2004), Vaughan and Pankhurst (2008), Ariza et al. (2018), and Creixell et al. (2021). Location of samples and their U-Pb crystallization ages are indicated according to (1) Hervé et al. (2014), (2) Deckart et al. (2014), (3) Maksaev et al. (2014), (4) del Rey et al. (2016), and (5) Jorquera et al. (2023). Estimated Frontal Cordilleran outline after Ramos et al. (2002) and Rossel et al. (2016).

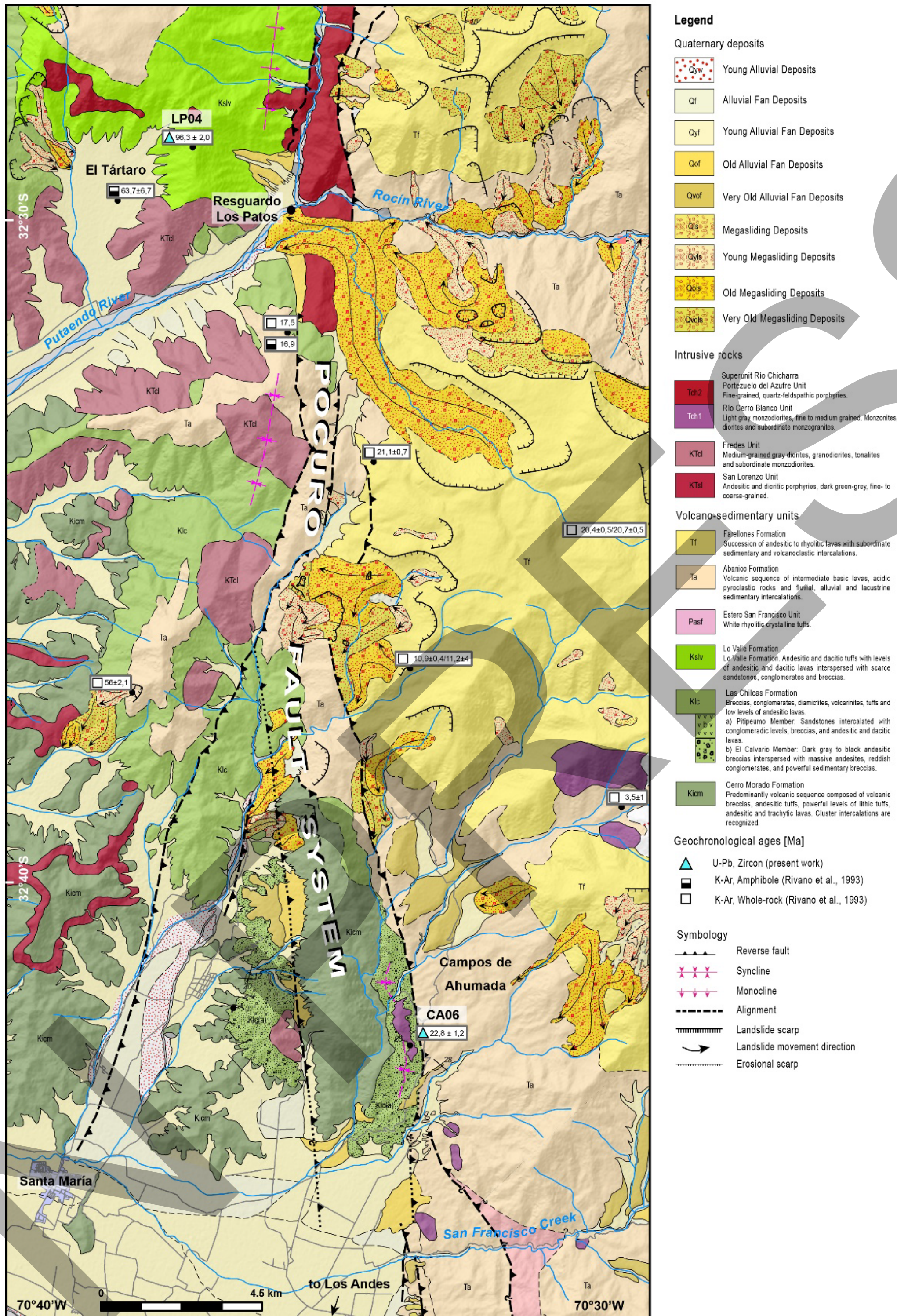

Fig. 2. Geological map and sample locations of the western border of the Principal Cordillera, around the Pocuro Fault system, where Carboniferous rocks are absent at the surface. Figure modified from Jackson-Gain (2023).

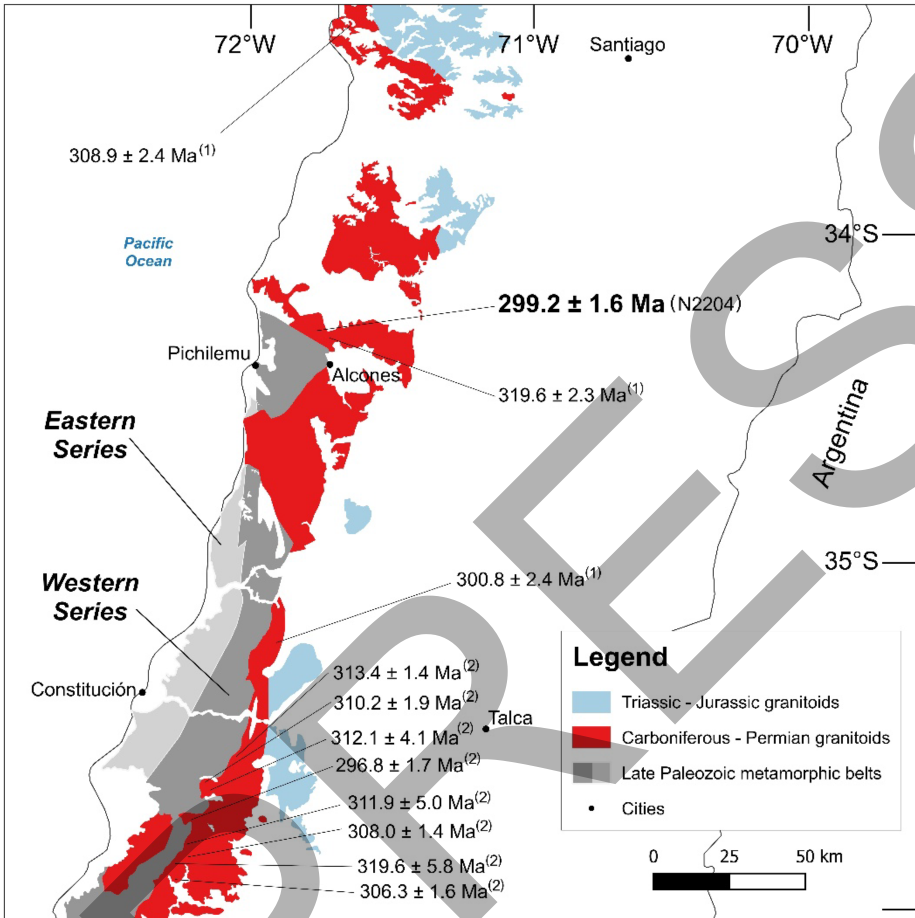

Figure 3

Fig. 3. Coastal Cordillera location map of sample N2204. Main age in bold. Other ages taken from (1) Deckart et al. (2014) and (2) Jorquera et al. (2023).

Figure 4

Fig. 4. CL images of selected zircon grains with marked spots (red circles) and respective ages of the LP04 crystalline tuff sample. See Table 1A for details.

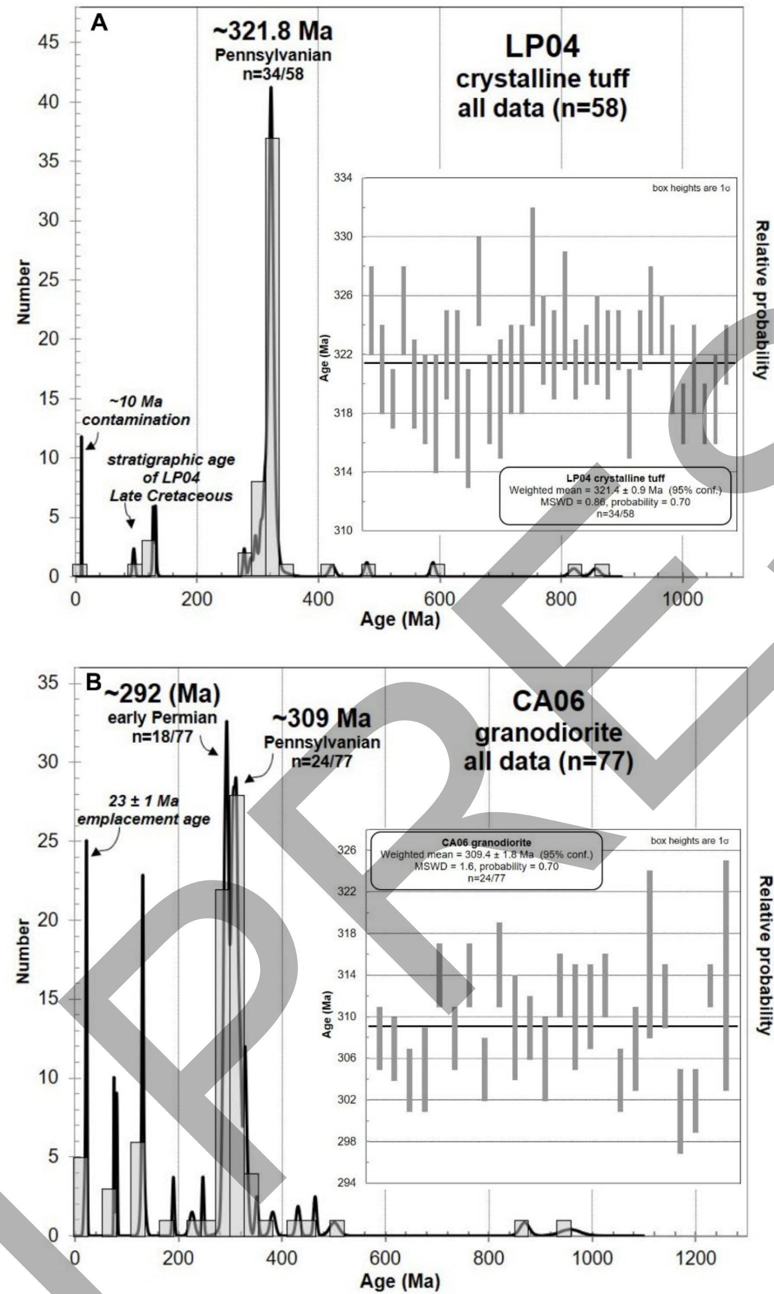
A
~321.8 Ma
Pennsylvanian
n=34/58
LP04
crystalline tuff
all data (n=58)
~10 Ma
contamination
stratigraphic age
of LP04
Late Cretaceous
box heights are 1σ
LP04 crystalline tuff
Weighted mean = 321.4 ± 0.9 Ma (95% conf.)
MSWD = 0.86, probability = 0.70
n=34/58
Age (Ma)
Number
Relative probability
B
~292 (Ma)
early Permian
n=18/77
~309 Ma
Pennsylvanian
n=24/77
CA06
granodiorite
all data (n=77)
23 ± 1 Ma
emplacement age
CA06 granodiorite
Weighted mean = 309.4 ± 1.8 Ma (95% conf.)
MSWD = 1.6, probability = 0.70
n=24/77
box heights are 1σ

Figure 5 A + B

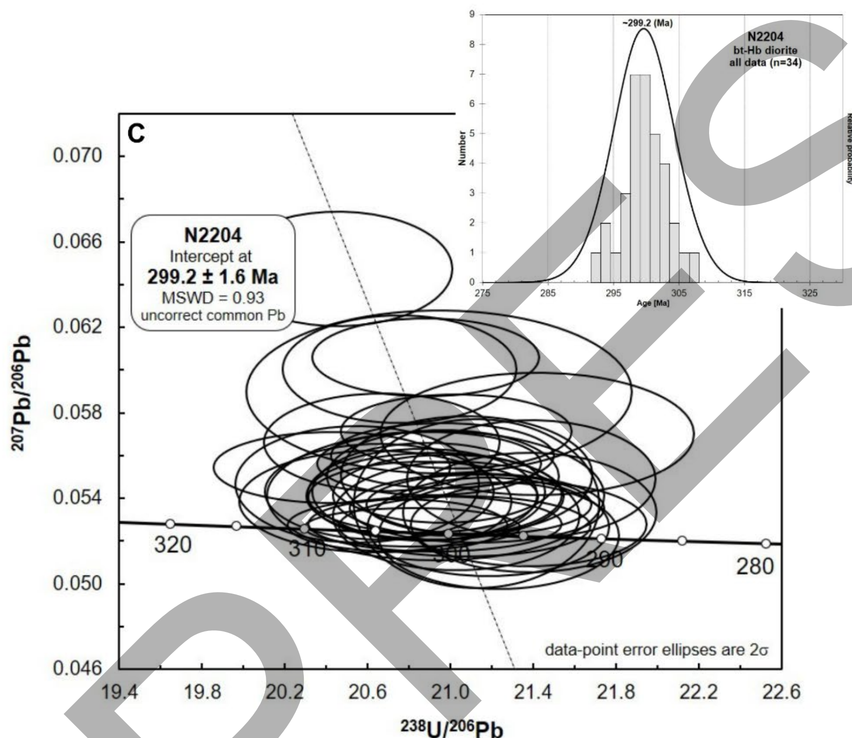

Figure 5C

Fig. 5. Relative probability plots combined with histograms for age distribution of zircon mineral sample. **A.** LP04 crystalline tuff with probable stratigraphic and inherited age information (Jackson-Gain, 2023). **B.** CA06 granodiorite with probable emplacement and inherited age information (Jackson-Gain, 2023). **C.** Common Pb (Pb_c) uncorrected concordia age spectrum with histogram of Pb_c corrected age distribution for N2204 biotite-hornblende diorite.

Figure 6.

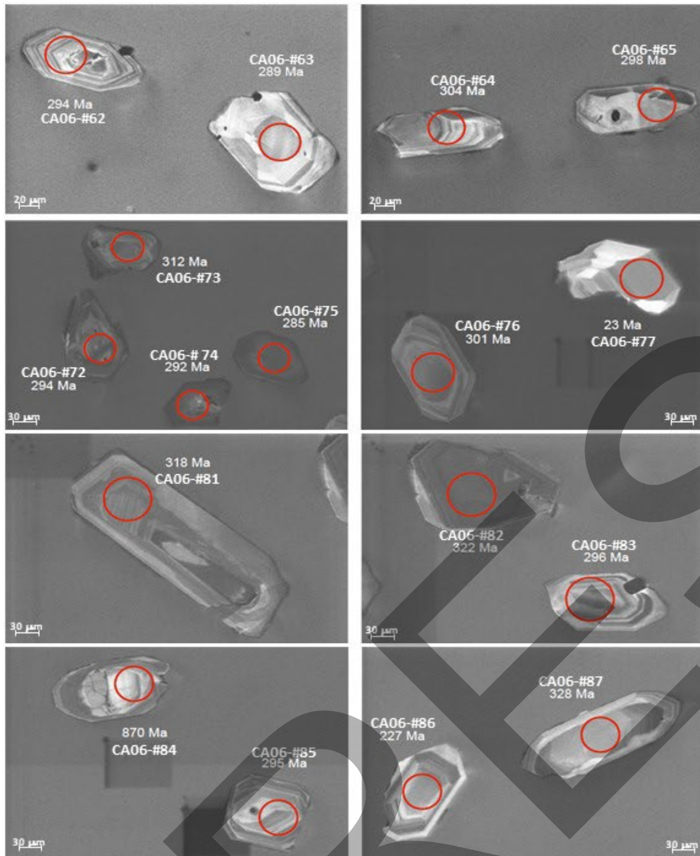

Fig. 6. CL images of selected zircon grains with marked spots (red circles) and respective ages of the CA06 granodiorite sample. See Table 1A for details.

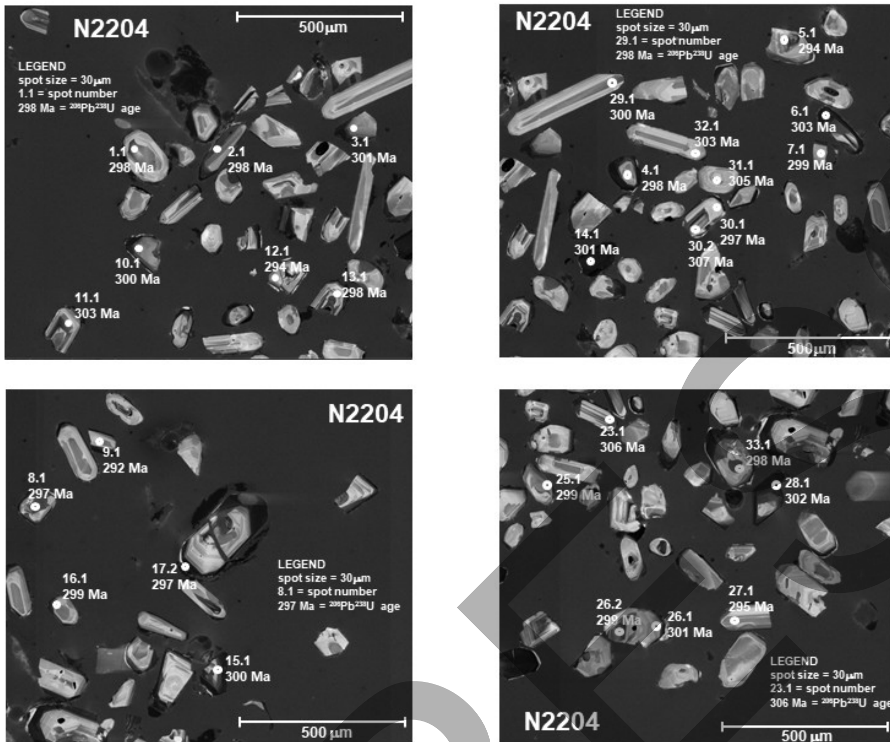

Figure 7

Fig. 7. CL images of selected zircon grains with ages of N2204 biotite-hornblende diorite sample. White circles refer to the analyzed spots and their respective ages. See Table 2 for details.

Table 1. Analytical U-Pb LA-ICP-MS data from samples LP04 (A) and CA06 (B). Western border of the Principal Cordillera.
Table 2. Analytical U-Pb SHRIMP data from sample N2204. Coastal Cordillera zone.

Supplementary Table 1. Analyzed standards for samples LP04 and CA06.
Supplementary Table 2. Analyzed standards for sample N2204.